

Effect of Accelerated Aging on the Structure and Properties of Monolayer and Multilayer Packaging Films

P. A. Tarantili, V. Kiose

Laboratory of Polymer Technology, School of Chemical Engineering, Sector IV, National Technical University of Athens, 9 Heroon Polytechniou Street, Zografou Campus, GR-15780, Athens, Greece

Received 2 November 2007; accepted 28 January 2008

DOI 10.1002/app.28091

Published online 1 April 2008 in Wiley InterScience (www.interscience.wiley.com).

ABSTRACT: The effect of accelerated aging on the structure and properties of single, metalized, and multilayer films used in food packaging was studied through the exposure of specimens of those films to repeated aging cycles in a weather meter under the combined action of ultraviolet, humidity, and heat. The aged specimens were tested for their mechanical properties and water vapor transmission characteristics, and the results were compared to those obtained from the original specimens. The property changes introduced into the films by aging were further explored by attenuated total reflectance spectroscopy and differential scanning calorimetry in an attempt to correlate the changes in the properties with structural characteristics. The results showed that the films made of polypropylene (PP) underwent severe chain scission upon irradiation and lost mechanical properties but still retained their impermeability to

water vapor. The metallic coating could not prevent PP from degrading, as it seemed to oxidize under the aging conditions. Therefore, the metalized film showed the same mechanical response as PP, but its water impermeability dropped dramatically. Polyethylene (PE) and poly(ethylene terephthalate) (PET) films showed modest decreases in their mechanical properties, which could be attributed to cross-linking reactions taking place with PE and to the increased ultraviolet stability of PET, respectively. On the other hand, the multilayer films presented a decrease in their mechanical properties according to those of their weak component, which would be expected for a composite structure. © 2008 Wiley Periodicals, Inc. *J Appl Polym Sci* 109: 674–682, 2008

Key words: ageing; films; mechanical properties; polyethylene (PE); poly(propylene) (PP)

INTRODUCTION

Multilayer coextruded or laminated flexible materials are a significant development in modern packaging technology. Their use finds ever increasing applications in the packaging of food, pharmaceuticals, medicine, cosmetics, and electronics because such materials combine a number of desirable properties, such as impermeability to gases and water vapor, mechanical strength, machinability, and relatively low cost.

There are many possible combinations of single materials in a coextrudate. Most coextruded multilayer structures are based on polyolefins because of their low cost, versatility, processability, chemical inertness, and high moisture-barrier properties, which are accompanied, however, by their poor ability to inhibit oxygen and aroma transmission. These multilayer structures are produced by the processing of commodity plastics such as polyethylene (PE) and polypropylene (PP), tie resins, and center barrier resins such as ethyl vinyl alcohol (EVOH) and polyamides through their respective extruders and a feed

block and then through a die to give five-layer films.^{1,2}

Polyamide resins are also an important class of polymers used in the packaging industry and owe their popularity to their good barrier properties against oxygen, aromas, and organic solvents along with high tensile strength and toughness.³

EVOH possesses excellent barrier properties to oxygen, aromatics, and oils. Oxygen diffusion through EVOH is limited by high intermolecular and intramolecular cohesive energy. However, this polymer is hygroscopic and absorbs water at an elevated relative humidity, and then it loses much of its oxygen barrier performance.⁴ Therefore, the use of coextrusion to combine PE and EVOH in a multilayer structure is a very attractive process for many demanding applications, such as for food, drugs, and cosmetics. Coextrusion, however, is often a very expensive procedure and requires a complex degree of control. Therefore, an alternative approach employing polymer blends appears more efficient for the design of products consisting of a barrier material and a polyolefin. The blend processing can occur in a single-step operation and offers process versatility and low cost. Dupont (Wilmington, DE) has developed blends of high-density polyethylene (HDPE) and nylon for packaging agricultural chemicals or making organic solvent con-

Correspondence to: P. A. Tarantili (taran@chemeng.ntua.gr).

tainers and fuel tanks. In addition, attempts at developing low-density polyethylene (LDPE)/EVOH and poly(ethylene terephthalate) (PET)/EVOH blends for food packaging films are in progress. Poly(vinylidene chloride) has also been proposed as a barrier polymeric film, but it is said to produce dioxins when it is burnt out at low temperatures.⁵

In addition to the aforementioned barrier properties, some other characteristics of polymer films must be taken into consideration for the proper design of a multilayered structure suitable for use in high-standard packaging. For instance, polymers are sensitive to several types of high-energy radiation, such as ultraviolet (UV) and gamma rays and electron and neutron beams. These external factors normally affect the surface at higher levels than the bulk of the polymer but nevertheless can have a great influence on the overall performance of these materials, depending on the absorbed dose and the final application. Aging caused by exposure to outdoor conditions is one of the most significant attacks leading to surface modification, and because of the small thickness of packaging films, it is obvious that its effect on their overall performance can be of great importance.⁶

The degradation of polymeric materials is initiated by various factors, such as heat, UV light, ozone, and mechanical stress, resulting in brittleness, cracking, color changes, and so forth. This procedure can then be promoted by oxygen, humidity, and strain. The degradation rates determined by laboratory tests can be extrapolated to predict the service life of a material under different conditions.

The greatest damage to polymers exposed to natural conditions is caused by the UV portion of sunlight, even though this portion represents up to 10% (depending on the atmospheric conditions and latitude) of the total energy reaching the earth from the sun, with about 50% of it being visible light and about 40% IR light.⁷

As generally accepted in the related literature, degradation reactions of semicrystalline polymers proceed predominantly in the amorphous regions; nevertheless, physical factors, such as the size, arrangement, and distribution of the crystalline regions, play an important role in the degradation process as well. The photodegradation kinetics in polymer systems basically depend on the oxygen permeability through the material. The rate of oxidation drops with decreasing oxygen diffusion, following the increase in the crystallinity and molecular orientation. Thus, the degradability of semicrystalline polymers can be significantly influenced by their supermolecular structure. It is worth noting that the photodegradation process is also affected by further parameters, such as the reactivity of the polymer, the presence of chromophoric impurities and addi-

tives, or conditions of accelerated aging or oxygen pressure.⁸

The study of the aging processes in polymers is of great importance for developing materials more resistant than those available in the past and for forecasting the limit of their use. In this work, single, metalized, and multilayer films used in food packaging were exposed to accelerated aging, and the changes in their properties were evaluated as a function of the exposure time. Attenuated total reflectance (ATR) spectroscopy and differential scanning calorimetry (DSC) measurements were also performed to detect the structural changes taking place upon aging. The investigation of interrelations between structural changes and those of final properties is undoubtedly a useful step in exploring the degradation mechanism and protecting films to extend their life cycle.

EXPERIMENTAL

Materials

The films investigated in this study were as follows:

1. Biaxially oriented polypropylene (BOPP) film, 40 μm thick, transparent, and produced by the tenter process (Diaxon SA, Komotini, Greece).
2. Film of biaxially oriented polypropylene metalized *in vacuo* (met-BOPP), 20 μm thick (Diaxon).
3. PE, 50 μm thick (Flexopack, Koropi, Greece).
4. PET, 12 μm thick (Nuroll Spa, Pignataro Maggiore, Italy).
5. Laminated PE with PET (PE/PET) film, 62 μm thick (Vlahos Br. SA, Koropi, Greece).
6. Coextruded PE/EVOH/PE film, 70 μm thick (Flexopack, Koropi, Greece).

Methods of testing

Accelerated aging process

Samples from the aforementioned films were exposed to an accelerated aging environment with the appropriate weather-meter chamber (type QUV weathering testers, Q-Panel, Lab Products, Cleveland, OH).

The aging tests were run according to ASTM D 4587-01⁹ and ASTM D 4329-99.¹⁰ Specimens were exposed to repeated cycles in which exposure to UV radiation and damp heating took place. The UV radiation was produced with a UVB-313 type lamp. Water in the bottom of the test chamber was heated, filling the chamber with hot vapor and creating 100% humidity at 50°C.

The specific setup of the accelerated aging procedure performed in this work was as follows:

1. Eight hours of UV radiation with a power of 0.76 W/(m²·nm) at 60 \pm 2.5°C.

2. Four hours of water condensation at $50 \pm 2.5^\circ\text{C}$.

Measurements at shorter time intervals were also taken (e.g., 4 and 2 h, respectively) in the case of BOPP films, which showed poor resistance to aging after some preliminary experiments.

For the determination of changes in the chemical structure of the aged films, spectroscopic measurements were performed with a Nicolet (Madison, WI) model Magna IR 750 Fourier transform infrared (FTIR) spectrometer (deuterated triglycine sulfate detector, nichrome source, beam splitter, and KBr). A total of 100 scans were applied with a resolution up to 4 cm^{-1} . Spectra were obtained in the ATR mode with a standard ZnSe 45° flat-plate contact sampler (12 reflections; Spectra-Tech, Stamford, CT) on which samples of laminated BOPP films were placed (100 μL). Spectroscopic data were treated with the standard software (Omnic 3.1, Nicolet).

All spectra were smoothed with the automatic smooth function of the aforementioned software, which uses the Savitsky–Golay algorithm (five-point moving second-degree polynomial). After the procedure, the baseline was corrected with the automatic baseline correct function.

DSC

DSC measurements were run in a PerkinElmer (Shelton, CT) DSC4 differential scanning calorimeter to reveal further structural changes related to chain compaction, crystallinity, and so forth. Small pieces cut from the films, with weights ranging from 7 to 10 mg, were accurately weighed in an analytical balance and encapsulated in aluminum pans. The samples were heated from 30 to 200°C at a rate of $5^\circ\text{C}/\text{min}$ under nitrogen. The melting temperature and heat of fusion were calculated from the thermographs obtained during heating.

Tensile properties

Tensile tests were carried out according to the specifications of ASTM D 882-75b.¹¹ Ten specimens were cut from each film with their long axis parallel to the machine direction, and they were tested in an Instron (Buckinghamshire, UK) model 4466 tensiometer equipped with a load cell with a maximum capacity of 10 kN and operated at a grip separation speed of 50 mm/min. The dimensions of the specimen were a length of 12 cm, a width of 1.5 cm, and a thickness of 20 μm . The tensile properties were examined along the machine direction of the film. All measurements were run at 25°C .

Water vapor permeation tests

The water vapor permeability tests were performed according to the specifications of ASTM E 96-66,¹² which is designated for the determination of the rate of vapor permeation through a plastic membrane. Specimens cut from each of the films under investigation were placed and fixed with epoxy glue on the top of a glass beaker containing a desiccant (e.g., silica gel).

The beaker was then placed in a chamber with a constant temperature of 25°C and a constant relative humidity produced by a saturated aqueous solution of potassium sulfate (a 12% w/w aqueous solution of K_2SO_4 produces an atmosphere of 95% relative humidity).

The vapor permeation was evaluated from the weight increase in the beaker after the weighing of the beaker at different time intervals until the last four measurements remained constant.

For the calculation of the water vapor transfer rate (WVTR), we used the following equation:

$$\text{WVTR} = \frac{1}{A} \times \frac{dQ}{dt} \quad (1)$$

where A is the exposed area of the film and dQ/dt is the rate of weight increase.

RESULTS AND DISCUSSION

ATR spectroscopy

The ATR spectra of BOPP, PE, and PET were obtained because these films are the exposure surfaces of the multilayer structures studied in this work; therefore, changes taking place in those layers are the most significant.

BOPP

The patterns obtained by ATR spectroscopy corresponding to the original BOPP sample and BOPP samples exposed to accelerated aging conditions for different time intervals are presented in Figure 1.

In the pattern of the original BOPP sample, we can observe first bands in the range of $2954\text{--}2839\text{ cm}^{-1}$, which can be attributed to the absorption of the different aliphatic bonds, and second bands at 1456 and 1374 cm^{-1} , which are due to C—H bending vibrations of $-\text{CH}_2$ and $-\text{CH}_3$ groups, respectively. As the aging procedure proceeds, these bands become less intense because of the mechanism of photo-oxidative degradation, which causes homolytic scission of C—C bonds and, therefore, results in a decrease of the molecular weight of the polymeric chain.

After 24 h of irradiation, some small structural modifications occur, as indicated by the new peaks

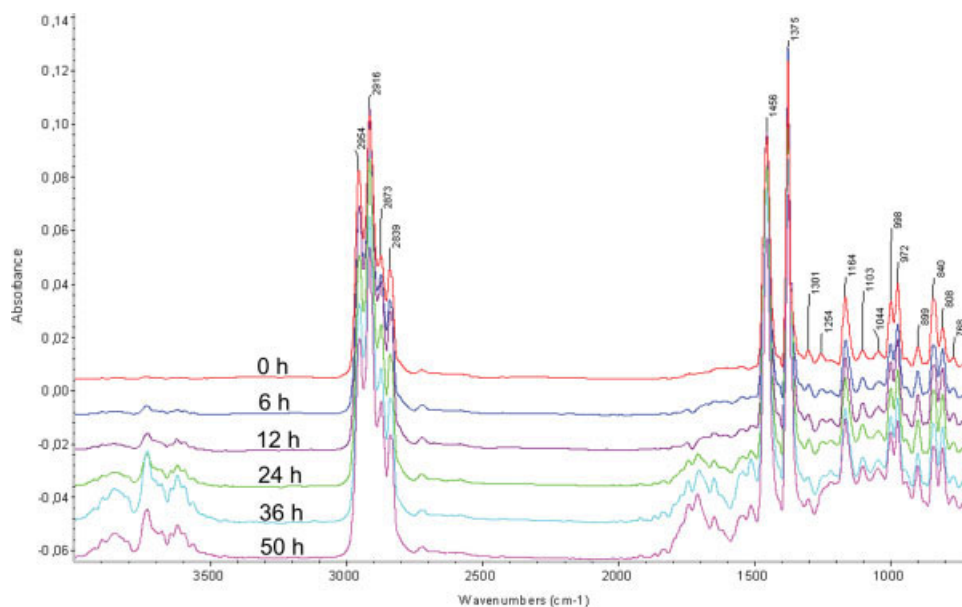


Figure 1 ATR absorption spectra of BOPP films before and after accelerated aging for different periods. [Color figure can be viewed in the online issue, which is available at www.interscience.wiley.com.]

appearing in the area from 1810 to 1665 cm^{-1} . These absorption bands indicate that more than one oxidation product is formed.

The photooxidation of a BOPP film taking place during accelerated aging can be estimated with the carbonyl index (CI_{BOPP}), which is calculated as the ratio of the area of carbonyl absorption bands in the range of 1810 – 1665 cm^{-1} ($A_{1810-1665\text{ cm}^{-1}}$) to the area of a reference band ranging from 2750 to 2700 cm^{-1} ($A_{2750-2700\text{ cm}^{-1}}$). The results for samples aged with different exposure times are shown in Figure 2, in which a rather linear dependence of this parameter with time is presented.

The shape of the carbonyl band is typically broad as it reflects several degradation products, including ketones, esters, and acids. On the other hand, the reference absorption peaks corresponding to C–H bending and $-\text{CH}_3$ stretching are narrow, and it is reasonable to assume that these bands are not associated with the photooxidation process and the variation of crystallinity.

According to Tidjani,¹³ ketones derived from peroxy radicals are the main photooxidation products under the natural and accelerated aging of PP films.

PE

The absorption spectra obtained from the ATR scans for PE films, before and after exposure to accelerated aging, are presented in Figure 3. It is clear that after 100 h of irradiation, some new absorption bands appear, which are related to the formation of the following:

- Double end bonds at 909 cm^{-1} .
- Branching at 1177 cm^{-1} .
- Ketone carbonyl groups at 1713 cm^{-1} , which is a measure of photooxidation.

Very interestingly, the band at 1645 cm^{-1} gradually fades, probably because of the migration of some additives taking place at the exposure temperature of 60°C or to breakage of double bonds present in PE.

The carbonyl index in the case of PE films (CI_{PE}) can be determined as the ratio of the integrated band absorbance of carbonyls around 1713 cm^{-1} ($A_{1713\text{ cm}^{-1}}$) to the absorbance of PE polymer bands at 1470 cm^{-1} ($A_{1470\text{ cm}^{-1}}$). The results for various aged samples are plotted in Figure 4 as a function of the exposure time. As expected, the curve of Figure 4

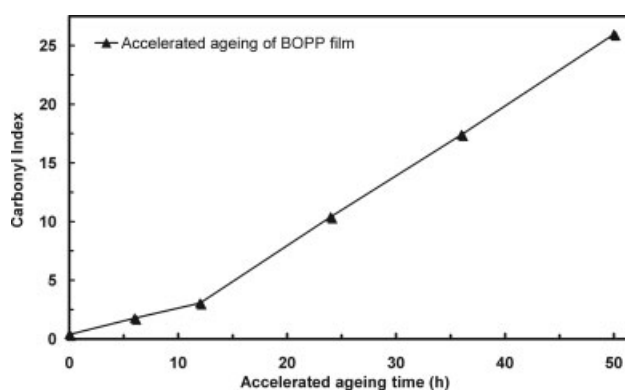


Figure 2 Propagation of the photooxidation of BOPP with the exposure time ($CI_{\text{BOPP}} = A_{1810-1665\text{ cm}^{-1}}/A_{2750-2700\text{ cm}^{-1}}$).

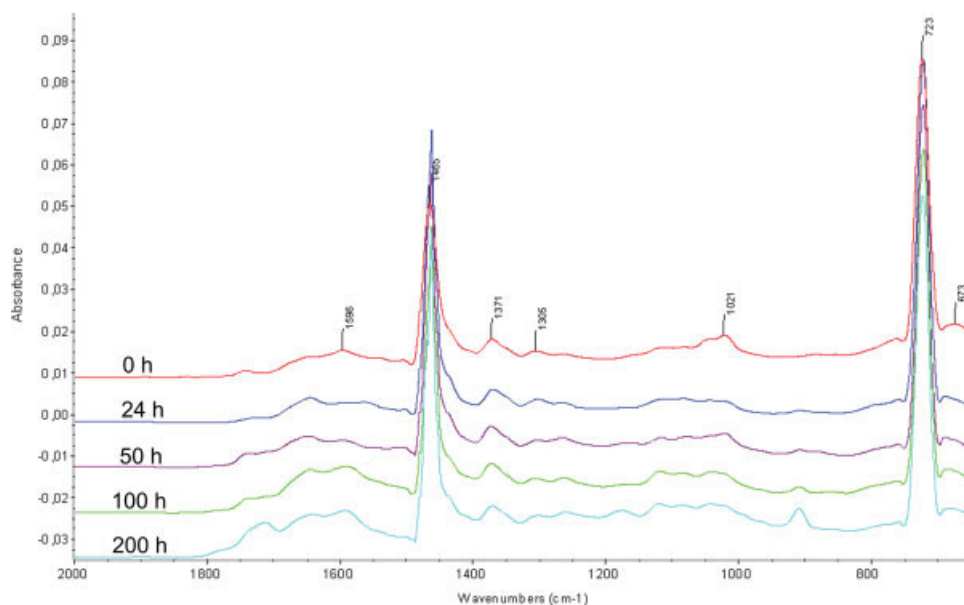


Figure 3 ATR absorption spectra of PE films before and after accelerated aging for different periods. [Color figure can be viewed in the online issue, which is available at www.interscience.wiley.com.]

shows an increase in photooxidation with aging, which becomes clear after 200 h of exposure. It should be noted, however, that the values of the carbonyl index for PE are much lower than those for BOPP, as can be seen by a comparison of Figures 2 and 4. Chain scission, branching, and oxidation after accelerated aging of HDPE exposed to UV irradiation were also observed by Carrasco et al.,¹⁴ who used FTIR analysis for their study.

PET

Similarly, Figure 5 shows the patterns obtained by ATR spectroscopy of PET before and after exposure to accelerated aging. Absorption at 3430 cm^{-1} is the overtone of the vibration of the carbonyl group at 1710 cm^{-1} , whereas the vibration of the C—H bond of the benzene ring occurs at $3100\text{--}3050\text{ cm}^{-1}$. Vibrations of C—H bonds corresponding to saturated aliphatic hydrocarbons create the peaks appearing at $2980\text{--}2900\text{ cm}^{-1}$. The strong carbonyl absorption occurs at 1716 cm^{-1} , and benzene ring absorptions are represented by the peaks at $1580\text{--}1500\text{ cm}^{-1}$. The ATR spectra of aged samples retain the same patterns as that of the original PET film, and this suggests that PET shows increased resistance to UV radiation.

DSC measurements

BOPP

The results derived from the thermographs obtained by DSC of BOPP film before and after exposure to

accelerated aging conditions are presented in Figure 6 and Table I. The heat of fusion, which is a measure of crystallinity, remains almost constant up to 50 h of exposure. However, after 100 h of irradiation, a significant increase is observed. This could be explained by the fact that UV aging of BOPP causes degradation and then the chain fragments can rearrange to better crystallize. As a result, the reduction of molecular weight leads to a lower melting point, whereas increased crystallinity corresponds to a higher heat of fusion.

Another important change observed in the DSC scans is a decrease in the melting temperatures, which obviously is the result of polymer degradation taking place via polymer chain scission or the photooxidation process.

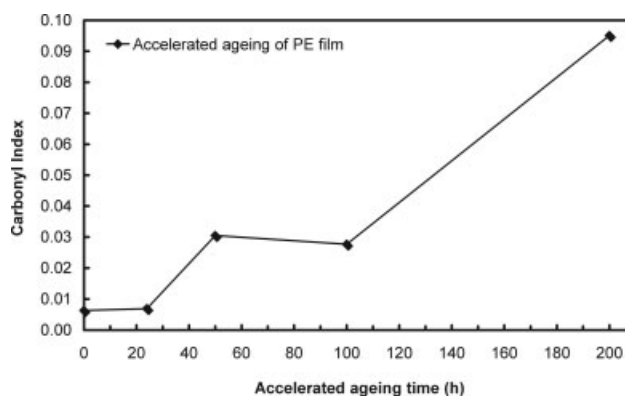


Figure 4 Propagation of the photooxidation of PE films with the exposure time ($CI_{PE} = A_{1713\text{ cm}^{-1}}/A_{1470\text{ cm}^{-1}}$).

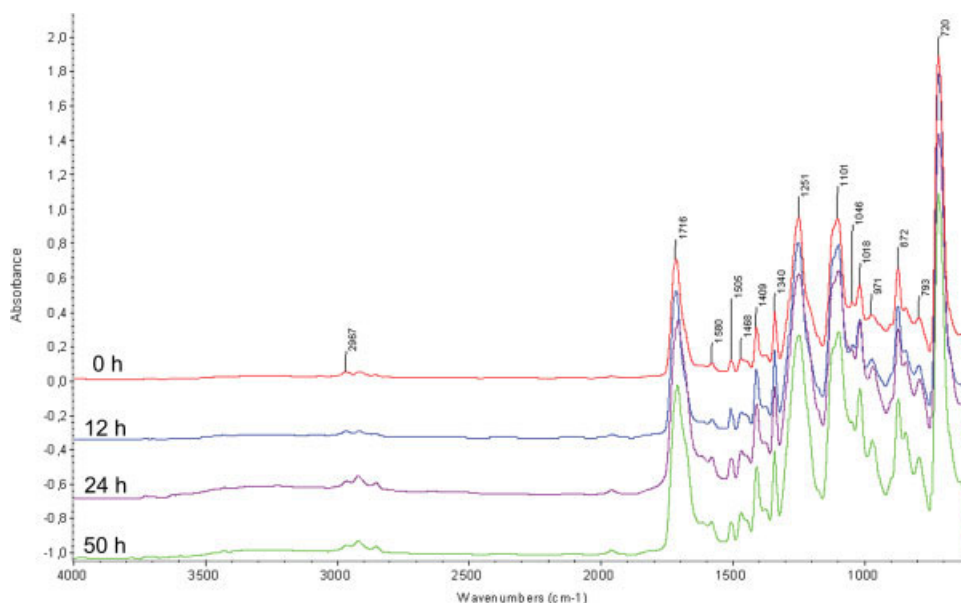


Figure 5 ATR absorption spectra of PET films before and after accelerated aging for different periods. [Color figure can be viewed in the online issue, which is available at www.interscience.wiley.com.]

PE

The DSC thermographs for aged PE mostly show that no essential changes in the polymer structure take place after irradiation, even though small variations in the content of crystallinity of UV-irradiated HDPE have been determined by the use of FTIR spectroscopy, and this effect has been attributed to complex structural and chemical changes.¹⁴

PET

For PET film, DSC measurements revealed that both the heat of fusion and melting temperatures significantly decrease with the time of exposure to the

combined action of humidity and UV radiation (Fig. 7 and Table II). This effect could be due to degradation phenomena during exposure to an accelerated aging environment.

Mechanical properties

The changes in the mechanical properties of the irradiated specimens, in terms of the tensile strength, elongation, and modulus of elasticity, at the end of the exposure to accelerated aging are shown in Table III. From the data of this table, it is clear that a significant drop in the mechanical properties of the films takes place upon their exposure to aging conditions. More specifically, the specimens become brittle after 200 h of irradiation, and this effect depends on the type of film. In fact, BOPP shows the maximum decrease in tensile strength and elongation, which is due to the vulnerability of PP to UV radiation. Very interestingly, the BOPP specimens show an increase in the modulus that can be attributed to the brittle-

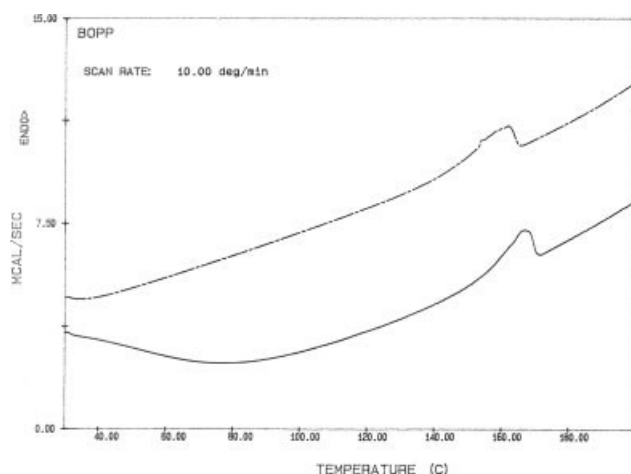


Figure 6 DSC thermographs of (—) a BOPP film and (---) a reference after 50 h of exposure to accelerated aging.

TABLE I
Data Obtained from the DSC Thermograph for Original and Aged BOPP

Accelerated aging time (h)	Melting temperature (°C)	Heat of fusion (cal/g)
0	166.1 ± 2.0	15.0 ± 0.8
6	167.3 ± 2.1	15.9 ± 2.3
12	163.9 ± 0.0	—
24	163.9 ± 1.0	16.6 ± 1.0
36	163.0 ± 1.1	14.6 ± 1.1
50	161.4 ± 0.8	16.7 ± 1.9
100	160.4 ± 1.9	19.3 ± 0.9

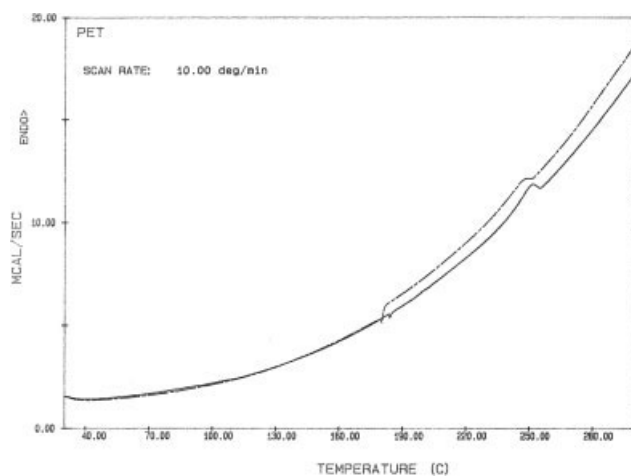


Figure 7 DSC thermographs of (—) a PET film and (---) a reference after 50 h of exposure to accelerated aging.

ness of the irradiated sample rather than to an increase of its stiffness. Similar behavior is presented by the met-BOPP film, which shows essentially the same changes as those of BOPP, despite the expected protective action of the metal coating on its surface. For an explanation of this effect, it is reasonable to assume that the film coating was oxidized by the combined action of UV radiation and humidity. It should be noted that most of the attacks in these two types of PP film took place within the first 50 h of exposure, as shown in Figure 8. Therefore, further study of these samples was impossible because of the loss of integrity of the related specimens. The aforementioned results are consistent with those derived from ATR spectroscopy, by which the main effect of aging of BOPP was found to be chain scission accompanied by photooxidation. Moreover, the information obtained by DSC analysis suggests that chain scission during the first 50 h of aging still allows the packing of polymer chain fragments; therefore, the crystallinity of BOPP remains constant within this period, whereas mechanical properties are seriously damaged. As the exposure to aging conditions proceeds, further scission of macromolecules and photooxidation of PP, introducing bulky groups into its chains, reasonably inhibit crystallization and result in a reduction of the heat of fusion.

TABLE II
Data Obtained from the DSC Thermograph for Original and Aged PET

Accelerated aging time (h)	Melting temperature (°C)	Heat of fusion (cal/g)
0	250.7 ± 0.4	6.1 ± 0.2
24	251.1 ± 0.1	5.6 ± 0.0
50	249.7 ± 0.6	5.1 ± 0.6
100	246.7 ± 0.4	3.8 ± 0.4

TABLE III
Tensile Properties of Different Types of Films

Film type	Tensile strength (%)	Modulus of elasticity (%)	Strain at break (%)
BOPP	-75	21.5	-99
met-BOPP	-78	17	-96
BOPP//met-BOPP	-82	-29	-96
PE	-22	15	-89
PET	-24	-24	-43.5
PE//PET	-65	-57	-86
PE/EVOH/PE	-40	-6	-75

In the related literature, the changes introduced to PP by multistress aging, including radiation, thermal, and electrical stress, were studied by Cygan and Laghari,¹⁵ who reported that mechanical properties undergo significant changes upon the exposure of the polymer to ionizing radiation and heat.

The effect of aging on the mechanical properties of PE shows a rather modest attack. As with BOPP, the tensile modulus of PE shows again an increase of 15%. In that case, however, an essentially smaller decrease in the tensile strength compared with that of BOPP can be observed, which is accompanied by a decrease of 89% in the elongation. These data probably suggest that some crosslinking takes place upon irradiation, which contributes to the increase of the modulus, whereas for BOPP, the main reaction introduced by UV is chain scission. This hypothesis is consistent with the data of Figure 8, in which the decrease in the tensile strength of PE proceeds very smoothly in comparison with that of BOPP; this might suggest the competitive action of chain scission and crosslinking. This can be further supported by the data obtained from the spectroscopic analysis. As already stated, the elimination of double bonds at 1645 cm^{-1} and the emergence of branching might be evidence for crosslinking. It also should be noted that Carrasco et al.¹⁴ studied effects of UV radiation on the mechanical properties of

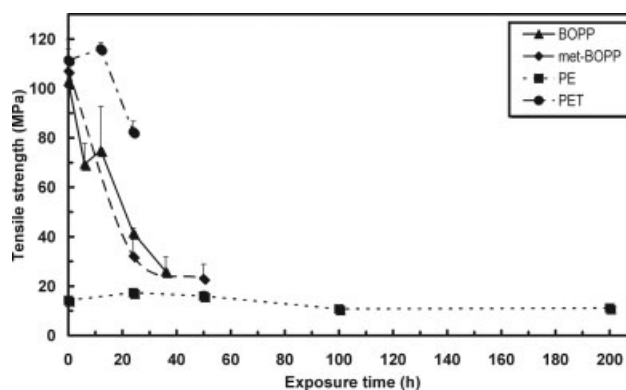


Figure 8 Tensile strength as a function of the accelerated aging time of various films.

HDPE and observed that Young's modulus increases with the irradiation time and the elongation at break shows a significant decrease. Moreover, those authors investigated irradiated samples via FTIR analysis and found evidence for branching and crosslinking. FTIR-ATR analysis was also used by Gulmine et al.¹⁶ to investigate chemical changes introduced into HDPE, LDPE, and linear LDPE. Those authors reported the possibility of the formation of a crosslinked structure. More specifically, they observed the creation of hydroperoxide radicals¹⁷ that could initiate crosslinking reactions during the irradiation of PE specimens. This discussion is consistent with the results obtained by the DSC scans of aged PE samples. In fact, chain scission and crosslinking allow the polymer chains to rearrange, so the crystallinity shows only small changes. On the other hand, a slight increase in the melting temperature of PE aged for 200 h can obviously be attributed to the crosslinked structure.

Behavior similar to that of PE can be seen with PET, for which modest decreases in the strength, modulus, and elongation are observed. This effect of aging can be attributed to the better UV stability of PET in comparison with that of polyolefins and particularly PP. The stability of PET was also reported by Jeon et al.,¹⁸ who studied the effect of γ -radiation on the physicomechanical properties of oriented PET films and found that permeability and thermal properties are not significantly affected. However, some other authors^{19,20} claim that PET needs protection with a UV absorber to retain its good properties. In addition to this, the sensitivity of PET to humidity must be taken into account, which could affect mechanical properties in the case of activation of a hydrolytic degradation process. However, Sun et al.²¹ reported that water absorption by PET simply produces reversible changes of its physical properties.²¹ The results from ATR spectroscopy are additional evidence, as only small changes in the absorption patterns were recorded.

On the other hand, the PE/PET system shows a much higher decrease in the strength and modulus, whereas its decrease in elongation is the same as that of the single PE film. This probably is the result of an early fracture of the PE layer during the tensile test due to its reduced elasticity. On the other hand, a serious attack of the tie resin between the layer of PE and PET by UV irradiation could also be possible, resulting in this mechanical response. Finally, the PE/EVOH/PE multilayer system shows again a higher decrease in the tensile strength and modulus in comparison with PE. This mechanical response can be attributed to the hydrophilic character of the inner layer of EVOH. In fact, this polymer can easily absorb water, and therefore the interfacial bonding between PE and EVOH is drastically reduced. In

TABLE IV
Water Vapor Permeability Measurements for Different Types of Films

Film type	Permeability $\times 10^{-4}$ (g cm/m ² /h/mmHg)	
	Before exposure	After exposure
BOPP	0.1103	0.1103
met-BOPP	0.0184	0.0735
PE	0.2574	0.2574
PE/PET	0.5130	0.6838
PE/EVOH/PE	0.2574	0.3217

addition, some failures at the interface due to degradation of the tie resin layer between the polymer films are also possible.

Permeability measurements

Table IV presents the water vapor permeability values of the six polymeric films. These measurements are valuable not only because they provide information about the material's performance during service but also because the changes in the permeability of the films can be directly related to their structural characteristics. From the data of Table IV, it can be clearly observed that no significant changes in the water vapor permeability values of BOPP take place upon prolonged exposure of the film to aging conditions. On the other hand, the metalized film shows a great increase in its permeability that obviously can be attributed to the destruction of the metal coating. In fact, this metallic layer works as a barrier and reduces drastically the permeability of BOPP, as can be seen in Table IV. However, after aging, its permeability increases by 4 times. The results observed for BOPP can also be observed for PE films, whereas the permeability values of PE/PET and PE/EVOH/PE increase 25 and 20%, respectively. As already stated, PET is susceptible to hydrolytic degradation, and EVOH is a hydrophilic polymer; therefore, the increase in water vapor permeability in these multilayer films can be attributed to hydrolytic attack of these two polymers during the aging procedure rather than to an attack by the UV light. This hypothesis is consistent with the data obtained by tensile testing of these films.

CONCLUSIONS

From the previous discussion, the following conclusions can be drawn. Accelerated aging is a simple and fast laboratory technique suitable for providing information about the performance of single and multilayer films used in packaging for service in outdoor applications. Moreover, when combined with mechanical testing, spectroscopy, and thermal analysis,

it can dictate the proper material selection and product design. The results of this work show that polyolefins are susceptible to degradation and photooxidation when exposed to aging conditions. PE, in contrast to PP, forms a crosslinked structure and therefore shows a modest decrease in its mechanical strength. On the other hand, PET shows good UV stability, whereas its resistance to water is low, and it undergoes hydrolytic degradation. EVOH was also found vulnerable to this attack.

The use of multilayer films requires special care with respect to the layer compatibility because after aging the failure mechanism can be promoted by the weak component of the systems. Finally, the UV and water stability of the interfacial tie resins placed between the film layers in a multilayer system to promote adhesion must also be taken into consideration for acceptable outdoor performance of the final products.

References

1. Kanai, T.; Campbell, G. A. *Film Processing*; Hanser: Munich, 1999.
2. Huang, C. H.; Wu, J.-S.; Huang, C. C. *Polym Int* 2004, 53, 2099.
3. Huang, C. H.; Wu, J. S.; Huang, C. C.; Lin, L. S. *Polym J* 2003, 35, 978.
4. Zhang, Z.; Britt, I. J.; Tung, M. A. *J Appl Polym Sci* 2001, 82, 1866.
5. Jang, J.; Lee, D. K. *Polymer* 2004, 45, 1599.
6. Tavares, A. C.; Gulmine, J. V.; Lepienski, C. M.; Akcelrud, L. *Polym Degrad Stab* 2003, 81, 367.
7. Jipa, S.; Setnescu, R.; Zaharescu, T.; Setnescu, T.; Kaci, M.; Touati, N. *J Appl Polym Sci* 2006, 102, 4623.
8. Obadal, M.; Čermák, R. V.; Raab, M.; Verney, V.; Commereuc, S. *Annu Tech Conf* 2006, 64, 782.
9. ASTM D 4587. *Annu Book ASTM Stand* 2001, v.06.01, 569.
10. ASTM D 4329. *Annu Book ASTM Stand* 2000, v.08.03, 325.
11. ASTM D 882-75b. *Annu Book ASTM Stand* 1977, v.35, 359.
12. ASTM E 96-66. *Annu Book ASTM Stand* 1977, v.35, 859.
13. Tidjani, A. *J Appl Polym Sci* 1996, 64, 2497.
14. Carraso, F.; Pagès, P.; Pascual, S.; Colom, X. *Eur Polym J* 2001, 37, 1457.
15. Cygan, S. P.; Laghari, J. R. *IEEE Transact Nucl Sci* 1991, 38, 906.
16. Gulmine, J. V.; Janissek, P. R.; Heise, H. M.; Akcelrud, L. *Polym Degrad Stab* 2003, 79, 385.
17. Küpper, L.; Gulmine, J. V.; Janissek, P. R.; Heise, H. M. *Vibr Spectrosc* 2004, 34, 63.
18. Jeon, D. H.; Lee, K. H.; Park, H. J. *Rad Phys Chem* 2004, 71, 1059.
19. Fechine, G. J. M.; Rabello, M. S.; Souto Maior, R. M.; Catalani, L. H. *Polymer* 2004, 45, 2303.
20. Lee, C. T.; Wu, C. H.; Lin, M. S. *Polym Degrad Stab* 2004, 83, 435.
21. Sun, N.; Yang, J.; Shen, D. *Polymer* 1999, 40, 6619.